

SOLAR POWERED SENSOR LESS BLDC MOTOR USING Z-SOURCE INVERTER

M.Jeeva, .P.Srividhya, Dr. C. Kumar

Power System Engineering,

SKP Engineering College,

Tamilnadu, India,

jeeva.me91@gmail.com sriviprakash2007@gmail.com drchkumararima@gmail.com

ABSTRACT

This paper proposes an implementation of Single Ended Primary Inductor Converter (SEPIC) and Z-Source Inverter for a Sensorless BLDC Motor using Photovoltaic energy as a source. SEPIC converter (DC-DC converter) with fuzzy logic control MPPT algorithm is used for matching the load and to obtain the PV module output voltage. With the help of ZSI the output voltage is used to run the BLDC motor at constant speed. This drive uses six switches which reduce the cost of the drive. And also the ZSI used for both inversion and boosting purpose. This utilizes the inductors and capacitors and the shoot through states by gating on both the upper and lower switches in the same phase legs, to boost dc voltage.

Keywords - Fuzzy logic controller; Maximum Power Point Tracking; Sensorless BLDC motor; Photovoltaic; SEPIC; Z-Source Inverter (ZSI).

1. INTRODUCTION

As the sources of conventional energy are dwindling fast with a corresponding rise in cost, considerable attention is being paid to other alternative energy sources. Solar energy which is free and abundant in most parts of the world has proven to be a challenging source of energy in many developing and developed countries. The solar energy as PV power systems can be operated as a standalone, hybrid or grid connected systems. The first schemes found a wide application in remote regions to meet small [1]. Photovoltaic (PV) water pumping systems have been increasingly popular in remote areas where grid is not accessible or is too costly to install. These systems are mostly used for agriculture and household purposes.

A number of dc motor driven PV pumps are already in use in several parts of the world. But they suffer from maintenance problems due to the presence of the commutator and brushes [2], [3]. Also some pumping systems based on induction motor have been proposed, where reliability and maintenance-free operations are important. Most low power motors such as single phase induction motors used for residential applications that drive low torque loads need to have a complex control drive system

[4], [5]. Having lower power range, simple structure and controllability, sensorless BLDC motors can be considered as a suitable alternative. Some early studies based on a BLDC motor have been one for PV water pumping system such as [6]. The investigation is based on boost converter which drives a BLDC motor. BLDC provide some advantages such as higher power density, higher efficiency and higher reliability. Therefore, BLDC offers a potential delegate for environmental protection and energy saving.

2. PHOTOVOLTAIC MODULE AND ARRAY MODEL

The model of solar cell can be categorized as p-n Semiconductor junction. When exposed to light, the DC current is generated. As known by many researchers, the generated current depends on solar irradiance, temperature, and load current. The typical equivalent circuit of PV cell is shown in Fig. 1. The basic equations describing the I-V characteristic of the PV model are given in the following equations:

$$0 = I_{sc} - I_d (e^{-V_d/V_t} - 1) - I_{pv}$$

$$I_d = I_o (e^{V_d/V_t} - 1)$$

$$V_{pv} = V_d - R_s I_{pv}$$

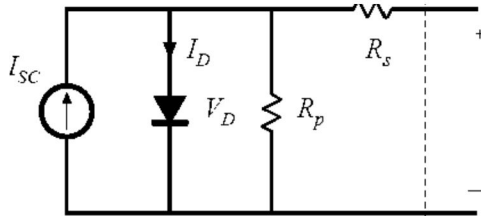


Figure. 1 Typical circuit of PV solar cell

Where:

- I_{pv} is the cell current (A).
- I_{sc} is the light generated current (A).
- I_D is the diode saturation current (A).
- R_s is the cell series resistance (Ω)
- R_p is the cell shunt resistance (Ω)
- V_d is the diode voltage (V).
- V_t is the temperature voltage (V).
- V_{pv} is the cell voltage (V).

3. PROPOSED ALGORITHM

MPPT Methods

There is a large number of algorithms that are able to track MPPs. Some of them are simple, such as those based on voltage and current feedback, and some are more complicated, such as perturbation and observation (P&O) or the incremental conductance (IncCond) method. They also vary in complexity, sensor requirement, speed of convergence, cost, range of operation, popularity, ability to detect multiple local maxima, and their applications [9],[10],[11].

On the other hand, some MPPTs are more rapid and accurate and, thus, more impressive, which need special design and familiarity with specific subjects such as fuzzy logic [12] or neural network [11] methods. MPPT fuzzy logic controllers have good performance under varying atmospheric conditions and exhibit better performance than the P&O control method [12].

MPPT Fuzzy Controller Design

MPPT fuzzy controller was designed and simulated using the Simulink Fuzzy Logic Simulink Toolbox represented in (Fig.2):

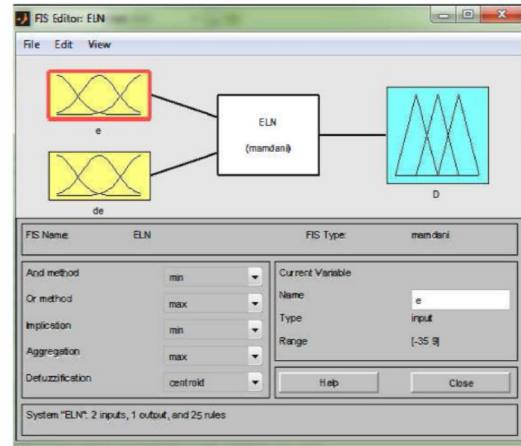


Figure. 2 General diagram of fuzzy controller MPPT MATLAB

The Fuzzy Logic tool is a mathematical tool for dealing with uncertainty. It offers to a soft computing partnership, the important concept of computing with words. It provides a technique to deal with imprecision and information granularity. The structure of fuzzy controller is shown in Fig.3.

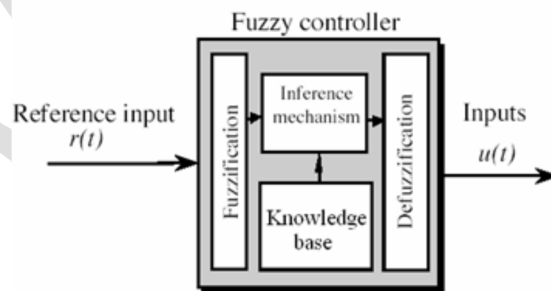


Figure. 3. Structure of fuzzy controller

1) Fuzzification

The values of membership function are assigned to the linguistic variables using seven fuzzy subsets called negative big (nb), negative medium (nm), negative small (ns), zero (zr), positive small (ps), positive medium (pm), and positive big (pb). Variables, change in voltage, dV and change in current, dI are selected as input variables and duty cycle, d is selected as output variable.

2) Inference Engine

Inference engine mainly consists of two-sub blocks namely, fuzzy rule base and fuzzy implication. The inputs which are now fuzzified are fed to the inference engine and the rule base is then applied; the output fuzzy sets are then identified using fuzzy implication method. The commonly used fuzzy implication method is MIN-MAX. The consequent fuzzy region is restricted to the minimum (MIN) of the predicate truth while selecting output fuzzy set. The output fuzzy region is updated by taking the maximum (MAX) of these minimized fuzzy sets during shaping of output fuzzy space.

3) Defuzzification

After fuzzy implication, output fuzzy region is located. As the final desired output is a non-fuzzy value of control, a defuzzification stage is needed. Center of gravity defuzzification method is used for defuzzification in the proposed scheme. In this method the weighted average of the membership function or the center of gravity of the area bounded by the membership function curve is computed as the most typical crisp value of the union of all output fuzzy sets.

4. SEPIC CONVERTER

When proposing an MPP tracker, the major job is to choose and design a highly efficient converter, which is supposed to operate as the main part of the MPPT. The efficiency of switch-mode dc-dc converters is widely used. Most switching-mode power supplies are well designed to function with high efficiency.

Among all topologies available, the single-ended primary inductance converter (SEPIC) is a DC/DC-converter topology that provides a positive regulated output voltage from an input voltage that varies from above to below the output voltage. It operates in continuous, discontinuous, or boundary conduction mode. SEPIC is controlled by the duty cycle of the control transistor. SEPICs are useful in applications in which a battery voltage can be above and below that of the regulator's intended output.

As with other switched mode power supplies specifically DC-to-DC converters, the SEPIC exchanges energy between the capacitors and inductors in order to convert from one voltage to another. A simple circuit diagram of a SEPIC converter is shown in Fig. 4, consisting of a coupling capacitor, C1 and output capacitor, C2; coupled inductors L1 and L2 and diode.

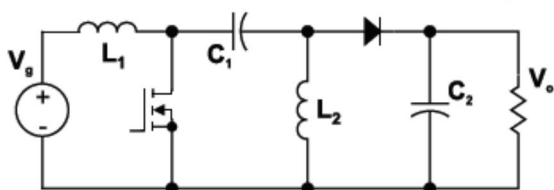


Figure. 4. Simple circuit diagram of SEPIC converter

Fig. 5 shows the circuit when the power switch is turned on. The first inductor, L1, is charged from the input voltage source during this time. The second inductor takes energy from the first capacitor, and the output capacitor is left to provide the load current. No energy is supplied to the load capacitor during this time. Inductor current and capacitor voltage polarities are also marked.

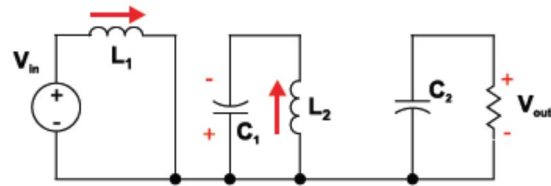


Figure. 5 SEPIC converter when switched ON

When the power switch is turned off, the first inductor charges the capacitor C1 and also provides current to the load, as shown in Fig. 6. The second inductor is also connected to the load during this time. The output capacitor sees a pulse of current during the off time, making it inherently noisier than a buck converter.

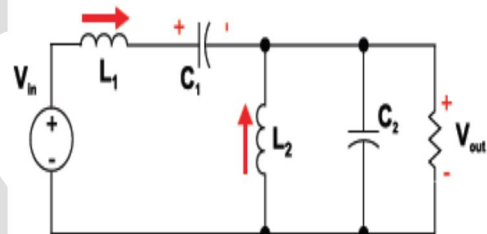


Figure. 6. SEPIC converter when switched OFF

The formulae of duty cycles is given as follows:

$$D_{min} = \frac{V_{OUT} + V_D}{V_{IN(max)} + V_{OUT} + V_D} \quad (1)$$

$$D_{max} = \frac{V_{OUT} + V_D}{V_{IN(min)} + V_{OUT} + V_D} \quad (2)$$

5. Z- SOURCE INVERTERS

The operation of a Z-source inverter [7] can be demonstrated with the help of a simplified circuit diagram, depicted in Fig.1 wherein a Z-source network is interposed between the PV panel and the semiconductor switches of the inverter. The Z-source network employs two inductors (L1 and L2) and two capacitors (C1 and C2) that are connected in 'X' shape [7]. As compared to VSI and CSI, a Z-source inverter has three modes of operation – active state, zero state and an additional shoot-through state.

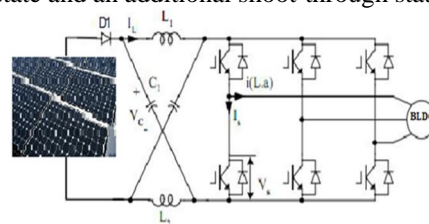


Figure. 7. System configuration using the Z-source inverter.

This additional shoot-through state provides the boost feature to the Z-source inverter. Active state occurs when any three switches from the upper and lower phase legs (but not from the same phase leg at a time) become ON. During zero state, all the three switches either from the upper leg or all from lower leg remain ON. Shoot through state occurs when any two switches of the same phase leg become ON. Since L1 and L2 are identical so as C1 and C2, it is obvious that Z-source network is symmetrical.

6. HYSTERESIS CURRENT CONTROL PWM

The reference current is generated and the actual current is detected by current sensors that are subtracted for obtaining current errors for a hysteresis based controller. The hysteresis band controller circuit is developed as shown in Fig. 8. The reference and actual currents are the input to this circuit. These currents are compared within a hysteresis band which can be adjusted by potentiometer. The output of this controller is given to the delay circuit through opto-coupler and wave shaping circuits. The ON/OFF switching signals for IGBT of inverter are derived from hysteresis controller.

When the actual (measured) current is higher than the reference current, it is necessary to commutate the corresponding switch to get negative inverter output voltage. This output voltage decreases the output current and reaches the reference current. On the other hand, if the measured current is less than the reference current, the switch commutated to obtain a positive inverter output voltage. Thus the output current increases and it goes to the reference current. As a result, the output current will be within a band around the reference one.

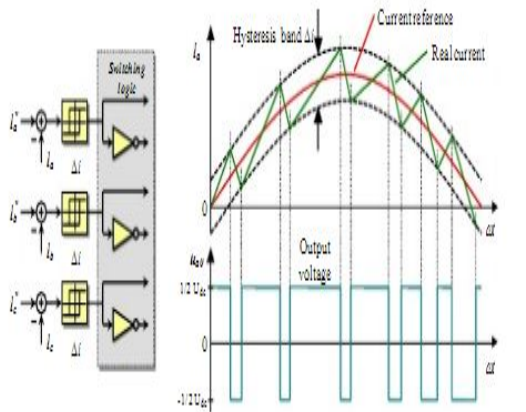


Figure.8 Hysteresis PWM – current control and switching logic

The switching function S_A for phase a is expressed as follows:

$$i_{sa} > (i_{sa}^* + HB) \rightarrow S_A = 1$$

$$i_{sa} < (i_{sa}^* - HB) \rightarrow S_A = 0$$

Where HB is a hysteresis current-band, similarly the switching function S_B, S_C can be derived for phases “b” and “c,” respectively. For hysteresis control the phase output current is fed back to compared with the reference current. An upper tolerance band and a lower tolerance band, taken as of, are also assigned in order to define an acceptable current ripple level. Whenever the phase current exceeds the upper band, the upper switch of that leg will be turned ON while the lower switch will be turned OFF. If phase current falls below the lower band, the upper switch will be turned OFF whereas the lower switch will be turned ON.

7. SIMULATION RESULTS

To evaluate the performance of the proposed system, simulation models have been established using MATLAB/simulink software. The fig. (9, 10, 11) shows the simulation results of BLDC motor output speed, Electromagnetic torque, The Inverter Output Voltage (V_{ab}) respectively.

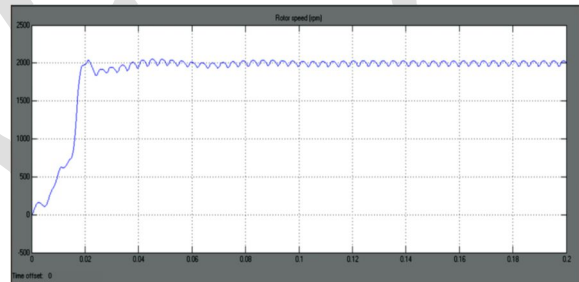


Figure.9. BLDC motor output speed

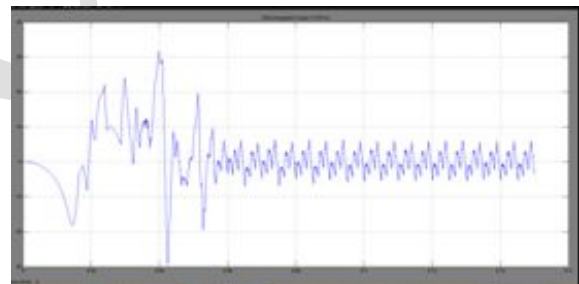


Figure10. Electromagnetic torque

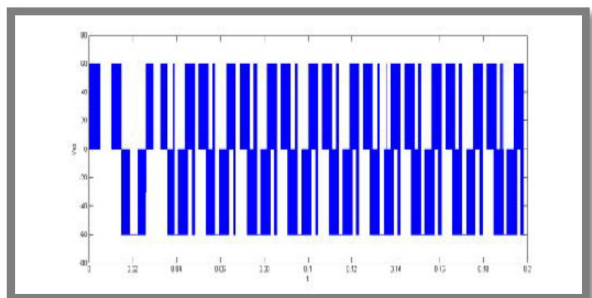


Figure 11. The Inverter Output Voltage (V_{ab}).

8. CONCLUSION

This paper presents the simulation work of a Photovoltaic array feeding a BLDC motor. SEPIC converter and z-source inverter were used as interface between PV module and the BLDC motor. Fuzzy logic controller algorithm was used to track the maximum power from PV module. The other main advantages of proposed MPPT method are no PV power oscillation and low torque ripple of BLDC motor. Indeed low torque ripple has been indirectly achieved by well voltage regulation of inverter at its reference value for the times after the system start up state. The simulation works of these circuits were carried out in the MATLAB/simulink software.

REFERENCES

- [1] I. Samin and et al, "Optimal sizing of Photovoltaic Systems in Varied Climates," Elsevier, Solar Energy, vol. 6, No. 2, 1997, pp.97-107.
- [2] C. Mummadi, "Steady State and Dynamic Performance Analysis of PV Supplied DC Motors Fed from Intermediate Power Converter," Elsevier Solar Energy Materials & Solar Cells, vol-61, 2000, pp. 365-381.
- [3] A Saadi And A Moussi, " Optimization of Chopping ratio of Boost converter by MPPT technique with a variable reference voltage applied to the Photovoltaic water Pumping System," IEEE ISIE.Conf2006, vol-7, 2000, pp. 1716-1720.
- [4] Arrouf M, Bouguechal N, "Vector control of an induction motor fed by a photovoltaic generator," Elsevier Applied Energy 2003; vol.74, issues 1-2, January-February 2003, pp.159-167.
- [5] MA Daud, M. Mahmoud, "Solar powered induction motor-driven water pumps operating on a desert well, simulation and field tests," Renewable Energy, vol. 30, issue 5, April 2005, pp.701-714.
- [6] R. Akkaya, A.A Kulakslz, O. Aydogdu, "DSP implementation of a PV system with GA-MLP-NN based MPPT controller supplying BLDC motor drive," Elsevier Energy Conversion and Management, vol. 48, issue 1, January 2007, pp. 210-218.
- [7] F. Z. Peng, "Z-source inverter", *IEEE Trans. Ind. Appl.*, vol. 39, no. 2, pp.504-510, Mar./Apr., 2003.
- [8] F. Z. Peng, M. Shen and Z. Qian, "Maximum Boost of Z-Source Inverter", *IEEE Trans. Power Electronics*, vol. 20, no. 4, pp. 833 - 838, July. 2005.
- [9] V. Salas, E. Olias, A. Barrado and A. Lazaro, 'Review of the Maximum Power Point Tracking Algorithms for Stand-Alone Photovoltaic Systems', *Solar Energy Materials & Solar Cells*, Vol. 90, N°11, pp. 1555 -1578, Jul. 2006.
- [10] W. Xiao, W. G. Dunford, P. R. Palmer, and A. Capel :*Regulation of photovoltaic voltage*. In *IEEE Trans. Ind. Electron.*, vol. 54, no. 3, pp.1365- 1374, Jun. 2007.
- [11] F. M. González-Longatt: *Model of photovoltaic module in Matlab*. In 2do congreso iberoamericano de estudiantes de ingeniería; a eléctrica, electrónica y computación, ii cibelec, 2005, pp. 1-5.
- [12] Z. Yan, L. Fei, Y. Jinjun, and D. Shanxu: *Study on realizing MPPT by improved incremental conductance method with variable step-size*. In *Proc. IEEE ICIEA*, Jun. 2008, pp. 547-550.
- [13] W. Wu, N. Pongratananukul, W. Qiu, K. Rustom, T. Kasparis, and I. Batarseh: *DSP-based multiple peak power tracking for expandable power system*. In *Proc. 18th Annu. IEEE Appl. Power Electron. Conf. Expo.*, Feb. 2003, vol. 1, pp. 525-530.
- [14] T.-F. Wu, C.-H. Chang, and Y.-H. Chen: *A fuzzy-logic-controlled single stage converter for PV-powered lighting system applications*. In *IEEE Trans. Ind. Electron.*, vol. 47, no. 2, pp. 287-296, Apr. 2000.